



Computational Study of Amino Acids, Order to Simulation of Membrane Protein Channels Using by Theoretical Methods

Reza Rasoolzadeh*

Young Researchers Club and Elites, Science and Research Branch, Islamic Azad University, Tehran, Iran

(Received 02 June 2013; revised manuscript received 02 August 2013; published online 31 August 2013)

The importance of ionic channels is due to the passage of ions across the cell membrane which is based on electrochemical gradients. The structure of ionic channels often includes one or several central cores which makes up the pore. The direct electron transfer between the enzyme and unmodified electrode is usually prohibited due to shielding of the redox active sites by the protein shells. In this paper, we have studied the stability of C60-amino acids clusters using by semi-empirical method and investigation of vibrational frequencies and electrical properties.

Keywords: Membranes proteins- membrane channels-, Amino acids- semi empirical.

PACS numbers: 87.15.kr, 87.15.ap

INTRODUCTION

Protein helices which make up the pore have consisted of four distinct subunits or one subunit which includes repetitive parts. Any disorder in protein-made channels causes paroxysm attacks. For instance, we can mention neuromuscular diseases as one type of these illnesses. These diseases are called disorders of ionic canals.

The function of channels is to allow selectivity and specificity for a Variety of molecular species transport across the cell membrane [1-4]. These channels, included: a) ligand-gated channels, b) voltage-gated channels, c) second messenger gated channels, d) mechanosensitive channels, e) Gap junctions: porins not gated [5-6].

The first step in understanding the physical mechanism of potassium transport through this protein nanopore is the determination of the water molecular distribution along the axial length of the pore Ion channels which are membrane proteins that mediation flux between the outside of the cell through a small, water-filled hole in the membrane-a pore. Ion- Selective pores were originally proposed to explain separate Components of Na⁺, K⁺ and leak currents in the classic experiments of Hodgkin and Huxley [7]. Potassium channels are the most diverse group of the ion channel family[1]. The recent determination of the crystallographic structure a bacterial K⁺ channel from streptomyces lividans (KcsA) [2] has provided the molecular basic for understanding the physical mechanisms Controlling ionic selectivity , permeation, and transport through Various types of K⁺ channels. [3-4].

In all cases, the functional K⁺ channel is tetramer [5], typically of four identical Subunits folded around a central Port [2]. Voltage – gated potassium (Kv) channels are members of the voltage – gated ion channel superfamily [1-2], which is important for initiation and propagation of action potentials in excitable cells. They are composed of four identical or homologous Subunits, each containing six transmembrane segments: S1-S6. Segments: S1-S4 form the voltage- sensing domain (VSD), and segments S5 and S6 Connected by the P loop, which

is involved in ion selectivity, Comprise the pore- forming domain (PD) S4 has four gating – charge- carrying arginines (R1-R4) spaced at intervals of three amino acid residues, which are highly conserved and are thought to play a key role in coupling changes in membrane Voltage to opening and closing of the pore [3-5]. In the Kv channels 13 electronic charges across the membrane electrical field per channel between the closed and open states [6-8]. Arginine residues interacting with lipid phosphate groups play an important role in stabilizing the voltage-Sensor domain of the KvAP channel within a bilayer. Simulations of the bacterial potassium channel kcsA reveal specific interactions of phosphatidylglycerol with an acidic lipid-binding site an the interface between adjacent protein monomers. Molecular and langevin dynamics simulation as well as Monte Carlo simulation have been used to investigate protein folding pathways with some success. The metropolis Monte Carlo was originally developed for calculating equilibrium properties of physical systems [9-12].The metropolis algorithm performs a sample of the configuration space of system starting from a random conformation and repeating a large number of steps. Molecular dynamics simulation is one the most promising approaches for solving the protein folding problem in this method we observe the time behavior of atoms of the system in MD simulation, new positions of atoms are calculated by numerical integration of newton's equation of motion [13-16].

The repentance of the existence of buckminsterfullerene C60 [17], theoretical speculation about carbon clusters [18] over 36 years was finally verified. Since then, this beautiful molecule has attracted ever more attention of theoretical and experimental scientists. Some chemists began to focus their research on the chemistry of this molecule, but real fullerene chemistry began only after 1990 when Kra'tschmer et al. described a method for preparing macroscopic quantities of C60 [19].

Direct electron transfer between the electrode and the redox enzyme is very important for fundamental studies and construction of biosensors [20-22]. However, the direct electron transfer between the enzyme and unmodified electrode is usually prohibited due to shield-

* Reza.Rasoolzadeh@yahoo.com

ing of the redox active sites by the protein shells [23, 24]. Therefore, several studies have been made to enhance the electron transfer. Mediators are widely used to access the redox center of an enzyme and then to act as the charge carriers. Mediators can minimize the effects of interferences, lower the operating potential of the electrodes, and improve the linear response range and sensitivity of the sensor [25]. Use of carbon nanotubes (CNTs) as mediators has attracted increasing attention in recent years. Comparing with traditional carbon electrodes, CNTs show unique properties, such as good conductivity, high chemical stability, and catalytic activities towards many electrochemical reactions [24, 26, 21, 27, 28]. More importantly, it is possible to bring the nanotubes close to the redox centers of the proteins [29, 30].

THEORETICAL BACKGROUND AND COMPUTATIONAL METHODS

Many studies have shown that the carbon nanotubes possess remarkable mechanical and physical properties leading to many potential applications such as fluid transport, fluid storage at nanoscale, and nanodevices for drug delivery. Since controlled experiments at the nanometer scale are very difficult, the simulation techniques have been widely and successfully used to investigate the mechanical property, wave propagation and resonant frequency [31]. The vibration of molecules is best described using a quantum mechanical approach. A harmonic oscillator does not exactly describe molecular vibrations. Bond stretching is better described by a Morse potential and conformational changes have sine-wave-type behavior. However, the harmonic oscillator description is very useful as an approximate treatment for low vibrational quantum numbers [32]. A harmonic oscillator approximation is most widely used for computing molecular vibrational frequencies because more accurate methods require very large amounts of CPU time. Frequencies computed with the Hartree-Fock approximation and a quantum harmonic oscillator approximation tends to be 10 % too high due to the harmonic oscillator approximation and lack of electron correlation [33]. The high-frequency oscillations encountered using flexible water models are of the order of 3500 cm^{-1} which are somewhat larger than the CNT vibrational modes of 1500 cm^{-1} [34]. Hence, for this case study, the use of the flexible water and solvent model.

Vibrational frequencies from semi-empirical calculations tend to be qualitative in (which) they reproduce the general trend mentioned in the Results here. However, the actual values are erratic. Some values will be close, whereas others are often too high. However PM3 is generally more accurate than AM1.

Since periodic boundary conditions cannot be adopted, first principles calculations of finite-length SWCNTs are only affordable to relatively small systems with C atom number less than 300 within our present computational ability [35].

The molecular mechanics method using the MM⁺ force field, and the Austin Model 1 (AM1) [36] and Parameterized Model number 3 (PM3) [37] semi-empirical method within the Restricted Hartree-Fock (RHF) formalism are sufficient to study carbon systems [38]. In 1989, Stewart improved the techniques of parameterization and published PM3, which gave lower average er-

rors than AM1, are sufficient to study carbon systems, mainly for the enthalpies of formation [37].

All calculations presented here were performed with semi-empirical Molecular mechanics (MM⁺) (Table 2).

In the first step of the calculations we optimized the geometry and defined Potential Energy of the nanotube structure by performing molecular mechanics calculation using MM⁺ force field, if too large a time step is used in monte carlo simulation, it is possible to have a basic instability in the equations that result in a molecule blowing apart, we need small time steps to preserve integration accuracy, however in the monte carlo time step 50 femtoseconds (0.05 ps) was appropriate.

In the next step we calculated the Vibrational modes of the tube by applying the semi-empirical molecular orbital method by the Hyperchem-7 package program [39].

RESULTS AND DISCUSSION

The resulting method was denoted, and in a sense, it is the best set of parameters (or at least a good local minimum) for the given set of experimental data. The optimization process, however, still requires some human intervention in selecting the experimental data and assigning appropriate weight factors to each set of data.

As a reference Table 1 is the result of semi-empirical computation using both method AM1& PM3.

At the first glance in Table 1, it can be observed by increasing dielectrics, normal modes will move to upper normal modes ratio and Vibrational frequencies resulted from semi-empirical Calculations tend to be qualitative.

Therefore by increasing dielectric the higher frequency will be gained in which semi-empirical methods will have the same operating procedure.

The PM3 and AM1 methods are also more popular than other semi-empirical methods due to the availability of algorithms for including salvation effects in these calculations. There are also some known strengths and limitations of PM3. Overall heats of formation are more accurate than with AM1. Hypervalent molecules are also predicted more accurately. On average, PM3 predicts energies more accurately than AM1.

The heats of formation are more accurate than AM1 or PM3 depending on the nature of the system and information desired, they will often give the most accurate obtainable results for organic molecules with semi-empirical methods. On average, PM3 predicts energies and geometries better than AM1.

There is energy of interaction in between solvent and solute. Therefore, the solute properties dependent on energy, such as geometry, total energy and vibrational frequencies depend on the solvent. The presence of a solvent, particularly a polar solvent, can also stabilize charge separation within the molecule. This not only changes the energy, but also results in a shift in the electron density and associated properties. In reality, these are the result of the quantum mechanical interaction between solvent and solute, which must be averaged over all possible attitudes of solvent molecules consistent with the principles of statistical mechanics. The results of the C60-aminoacids clusters simulation can be used to analyze the energetic aspects which are associated with the process of introducing a C60 fullerene from the gas phase into different amino acids (Table 2 and Fig. 1).

Table 1 – Calculated Properties of C60 and binding to amino acids

Atom number	C60 Ala- gly			Atomic number	C60 Ala- leu			Atom number	C60 Gln- asn		
	A	B	C		A	B	C		A	B	C
1	-18.293	6.77	-0.446	1	-18.301	7.33	-0.393	1	-18.264	6.30	-0.469
2	-14.653	7.79	-0.107	2	-14.673	7.85	-0.188	2	-14.664	7.48	-0.047
3	-14.621	9.10	0.337	3	-14.651	9.29	0.322	3	-14.666	7.53	0.339
4	-22.238	9.32	-0.285	4	-22.260	9.85	-0.310	4	-22.257	6.68	-0.386
5	-14.714	8.26	-0.413	5	-14.765	7.20	-0.399	5	-14.728	8.71	-0.236
14	-14.744	6.07	-0.207	6	-14.683	7.85	0.135	6	-14.733	9.94	-0.351
56	-14.657	5.75	0.027	7	-14.776	5.48	-0.172	7	-14.733	11.19	0.513
66	-18.404	9.75	-0.406	8	-18.382	8.94	-0.368	8	-22.361	11.23	-0.453
67	-14.735	8.57	-0.240	9	-14.714	7.86	-0.116	9	-18.329	12.34	-0.718
68	-14.690	7.36	0.358	15	-14.729	6.50	0.362	15	-14.776	6.32	0.020
69	-22.367	7.65	-0.429	69	-22.364	6.59	-0.452	69	-14.649	5.53	0.101
				70	-14.743	8.23	-0.231	70	-18.412	9.61	-0.423
				71	-14.735	7.38	-0.133	71	-14.726	8.39	-0.136
				72	-14.771	7.57	-0.389	72	-14.714	7.20	0.175
				73	-14.756	8.17	-0.395	73	-22.346	7.53	-0.320
								74	-14.728	8.61	-0.344
								75	-14.619	7.57	0.561
								76	-22.335	6.55	-0.470
								77	-18.309	8.02	-0.711
Normal mode	Frequency	Intensity			Frequency	Intensity			Frequency	Intensity	
	Max	225 A	1 A		261 A	6 A	267 A		1 A		
		2819.29	2971.76		2811.35	2151.43		3056.54	751.13		
ΔE	-2739.14				-2895.54				-3154.71		
Dipole moment	11.7590				3.2852				14.0020		

Table 2 – Semi empirical Calculations for C60 fullerene and conjunction to amino acids

Atom number	C60 Nanotube		
	A	B	C
1	-14.562	5.91621	0.049
2	-14.562	5.91621	0.050
5	-14.559	5.91623	0.053
6	-14.560	5.91621	0.051
9	-14.56	5.91624	0.052
10	-14.560	5.91625	0.052
51	-14.567	5.91618	0.068
52	-14.568	5.91619	0.061
55	-14.592	5.91619	0.040
56	-14.588	5.91617	0.045
59	-14.604	5.91634	0.022
60	-14.607	5.91634	0.025
Normal mode	Frequency	Intensity	
	Max	71 AU	2A
		1363.12	457.69
ΔE	-2283.99		
Dipole moment	4.1475		

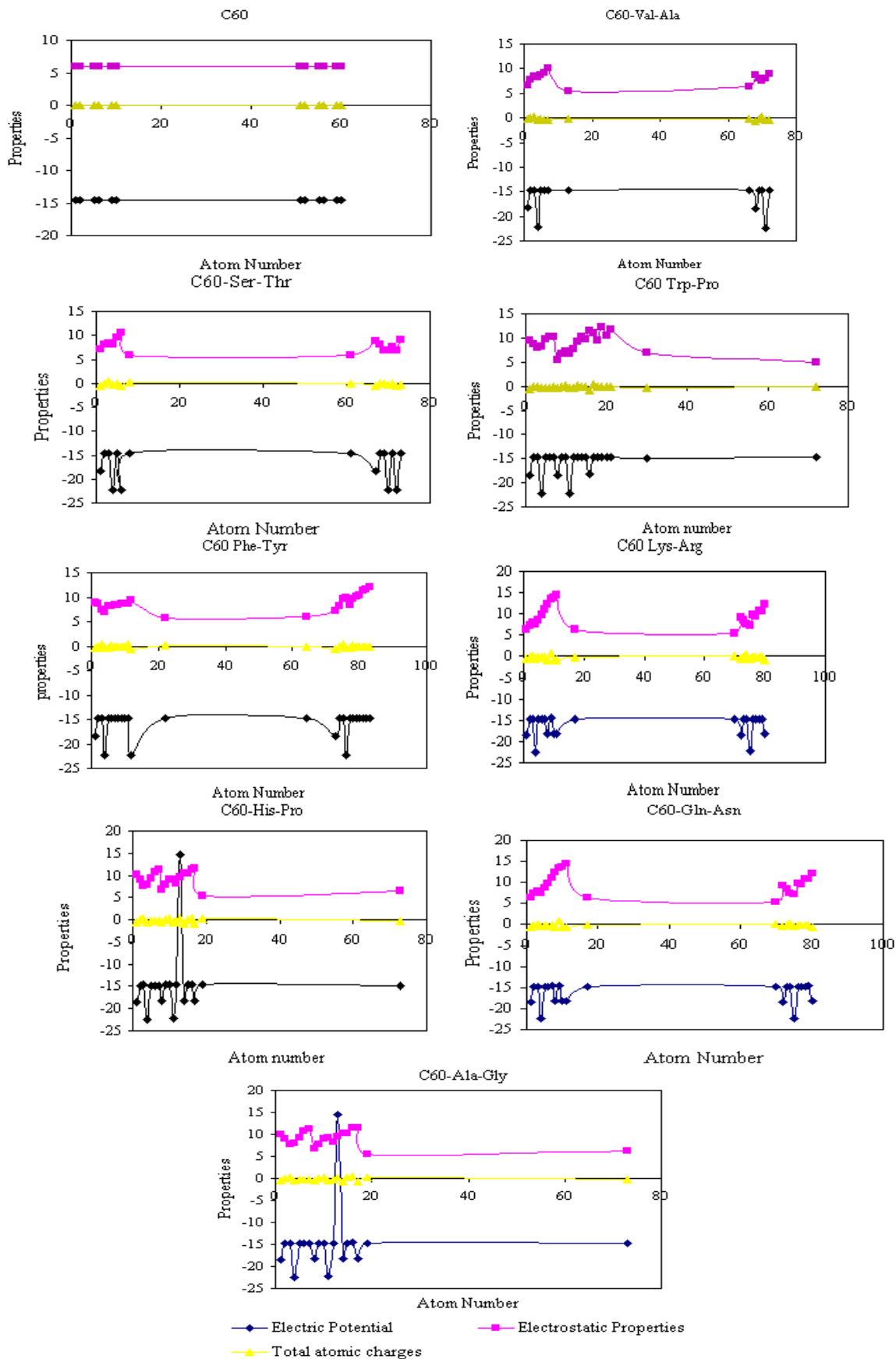


Fig. 1 – Plotting of Calculated Properties of C60 and binding to amino acids

The net result clearly indicates that the process of introducing a C60 to different amino acids energetically is remarkable.

Whereas a molecular mechanics potential used to characterize the response of a SWCNT which allows long range interactions between atoms, results in Molecular Mechanics force field which indicates that potential energy is maximum and also the potential energy will increase. (As shown in Table 2 and Fig. 1).

CONCLUSION

To reconstruct membranous proteins, we used simulated nanotubes in order to transfer ions across the membrane and transfer of ions was done successfully. In this study the more the potential energy increases the more the conductivity of nanochannels decreases and we chose the least energy among nanotube and amino acid

complexes. And also the more energy we use, the more conductivity we will have; therefore we choose the complex which conducts the most current. This way we can simulate the channels which have hereditary defects and are not efficient and observe the fundamental cure of the diseases.

According to the Conference policy, the proceedings will be published instead of the abstract book. The conference proceedings will be published up to the conference sessions for the convenience of the participants and the best dissemination through the Web, since the proceedings paper will be freely available on-line. In order to speed up the availability of your paper online, the submitted manuscript must be ready for publication. So, the strict requirements to the manuscript preparation exist.

REFERENCES

1. L.K. Kaczmarek, T.M. Perney, *Curr. Opin. Cell. Biol.* **3**, 663 (1991).
2. D.A. Doyle, J. Morais Cabral, *Science* **280**, 69 (1998).
3. L. Heginbotham, *Nat. Struct. Biol.* **6**, 811 (1999).
4. B. Hille, C.M. Armstrong, R. Mackinnin, *Nat. Med.* **5**, 1105 (1999).
5. R. Mackinnon, *Nature* **350**, 232 (1991).
6. B. Hille, *Ion channels of Excitable membranes* (2001).
7. S. Chone, *Potassium channel structures* (2002).
8. F.H. Yu, W.A. Catterall, *Sci. STKE* (2004).
9. S.B. Prusiner, *Science* **278**, 417 (1997).
10. H. Liu, M. Elstner, E. Kaxiras, T. Frauenheim, J. Hermans, Yang, *Quantum mechanics simulation of protein dynamics on long timescale Proteins: Structure, function, and Genetics* **44**, 484 (2001), 12. J.L. Popot, D.M. Engelman, *Annu. Biochem.* **69**, 881 (2000).
11. A.G. Lee, *Biochim. Biophys. Acta* **1666**, 62 (2004).
12. N. Metropolis, A.W. Rosenblth, M.N. Rosenblth, E. Teller, *J. Chem. Phys.* **21**, 1087 (1953).
13. Hs. Chans, K.A. Dill, *J. Chem. Phys.* **100**, 9238 (1994).
14. A. Kolinski, J. Skolnick, *Polymers* **45**, 511 (2004).
15. Hyperchem 8.0, Hype Cube Inc., Gainesville, FL, USA, 2007.
16. W. Humphrey, A. Dalk, K. Schulten, *J. Mol. Graphics* **14**, 33 (1996).
17. H.W. Kroto, J.R. Heath, S.C. O'Brien, R.F. Curl, *Nature* **318**, 162.
18. E. Dornenburg, H. Hintenberger, *Science Direct* **91**, 765 (1989).
19. W. Kratschmer, L.D. Lamb, K. Fostiropoulos, D.R. Huffman, *Nature* **347**, 354 (1990).
20. R. Liang, M. Deng, S. Cui, H. Chen, J. Qiu, *Biosensors, Bioelectron.* **45**, 1855 (2010).
21. F. Mollaamin, K. Shahani Poor, T. Nejdassattari, *African J. Microbiology Res.* **4**, 2098.
22. M. Albareda-Sirvent, A.L. Hart, *Anal. Chem.* **87**, 73 (2002).
23. Z. Wang, M. Li, P. Su, Y. Zhang, Y. Shen, D. Han, A. Ivaska, L. Niu, *Biosensors. Bioelectron.* **10**, 306 (2008).
24. F. Mollaamin, I. Layali, A.R. Ilkhani, M. Monajjemi, *African J. Microbiology Res.* **4**, 2795 (2010).
25. L. Zhang, R. Yuan, Y. Chai, X. Li, *Analytica Chimica Acta* **596**, 99 (2007).
26. Z. Wang, M. Li, P. Su, Y. Zhang, Y. Shen, D. Han, A. Ivaska, L. Niu *Biosensors. Bioelectron.* **10**, 306 (2008).
27. J. Manso, M.L. Mean, P. Ya'n'ez-Seden'o, J. Pingarro'n, *J. Electroanal. Chem.* **603**, 1 (2007).
28. K. Jurkschat, S.J. Wilkins, C.J. Salter, H.C. Leventis, G.G. Wildgooses, L. Jiang, T.G.J. Jones, A. Crossley, R.G. Compton, *Small* **2**, 95 (2006).
29. J.J. Gooding, R. Wibowo, J.Q. Liu, W.R. Yang, D. Losic, S. Orbons, F.J. Mearns, J.G. Shapter, D.B. Hibbert, *J. Am. Chem. Soc.* **125**, 9006 (2003).
30. J. Liu, A. Chou, W. Rahmat, M.N. Paddon-Row, J.J. Gooding, *Electroanalysis* **17**, 38 (2005).
31. Toshiaki Natsukia, Qing-Qing Ni, Morinobu Endo, *Carbon* **46**, 1570 (2008).
32. Youky Ono, Nobuhiro Kusuno, Koichi Kusakabe, Naoshi Suzuki, *Jpn. J. Appl. Phys.* **48**, 045001 (2009).
33. H. Fangohr, Bhaskar, *J. Phys.: Conf. Ser.* **26**, 131 (2006).
34. J.H. Walther, R. Jaffe, T. Halicioglu, P. Koumoutsakos, *J. Phys. Chem. B* **105**, 9980 (2001).
35. Shaojie Ma, Wanlin Guo, *Phys. Lett. A* **372**, 4835 (2008).
36. M.J.S. Dewar, E.G. Zoebisch, E.F. Healy, J.J.P. Stewart, *J. Am. Chem. Soc.* **107**, 3902 (1985).
37. J.J.P. Stewart, *J. Comput. Chem.* **10**, 209 (1989).
38. S Akir Erkoc, *Physica E* **25**, 69 (2004).
39. Hypercube, Inc., Gainesville, FL, USA.

Notes: (A) Electric Potential, (B) Electrostatic Properties, (C) Total atomic charges

Atom Number	C60 His-Pro			Atom ic number	C60 Lys-Arg		
	A	B	C		A	B	C
1	-18.421	10.12	-0.502	1	-18.340	6.28	-0.593
2	-14.757	8.93	-0.054	2	-14.753	7.43	-0.065
3	-14.713	7.67	0.321	3	-14.769	7.96	0.178
4	-22.380	7.92	-0.414	4	-22.375	7.54	-0.398
5	-14.800	9.29	-0.253	5	-14.751	8.66	-0.255
6	-14.798	10.82	-0.276	6	-14.732	9.86	-0.282
7	-14.769	11.22	-0.140	7	-14.652	11.10	-0.120
8	-18.322	6.66	-0.608	8	-18.228	12.30	-0.649
9	-14.690	7.78	-0.063	9	-14.496	13.51	0.863
10	-14.702	9.04	0.182	10	-18.215	13.80	-0.728
11	-22.316	9.14	-0.392	11	-18.218	14.54	-0.741
12	-14.694	8.25	-0.288	17	-14.771	6.44	-0.159
13	-14.619	9.55	0.276	70	-14.761	5.38	0.052
14	-18.192	10.31	-0.679	72	-18.513	9.18	-0.514
15	-14.633	10.36	0.149	73	-14.797	8.59	-0.123
16	-14.564	11.42	0.411	74	-14.728	7.48	0.371
17	-18.187	11.46	-0.679	75	-22.350	7.22	-0.447
19	-14.698	5.48	0.186	76	-14.795	9.74	-0.236
73	-14.774	6.36	-0.217	77	-14.778	9.46	-0.234
				78	-14.718	10.81	-0.271
				79	-14.637	10.84	-0.207
				80	-18.155	12.24	-0.680
Normal mode Max	Frequency		Intensity		Frequency		Intensity
	273 A		1 A		1 A		2 A
	2997.06		250285.34		6967.70		776150.43
ΔE	-3082.21				-3235.42		
Dipole moment	32.3063				33.2251		

Notes: (A) Electric Potential, (B) Electrostatic Properties, (C) Total atomic charges

Atom number	C60 Ser-Thr			Atomic number	C60 Val-Ala		
	A	B	C		A	B	C
1	-18.30	7.14	-0.50	1	-18.28	6.52	-0.25
2	-14.67	8.09	-0.10	2	-14.65	7.76	0.02
3	-14.64	8.44	0.36	3	-14.64	8.55	0.33
4	-22.23	7.99	-0.25	4	-22.25	8.26	-0.33
5	-14.67	9.46	-0.01	5	-14.71	8.78	-0.12
6	-22.31	10.44	-0.59	6	-14.73	9.20	-0.42
8	-14.71	5.85	0.30	7	-14.74	10.07	-0.40
61	-14.69	5.97	0.03	13	-14.69	5.52	-0.24
67	-18.42	8.89	-0.46	66	-14.73	6.28	-0.10
68	-14.70	8.05	-0.12	68	-18.39	8.64	-0.63
69	-14.68	6.94	0.04	69	-14.72	7.89	-0.11
70	-22.30	6.94	-0.34	70	-14.69	7.51	0.31
71	-14.64	7.63	-0.03	71	-22.35	7.89	-0.40
72	-22.17	6.91	-0.47	72	-14.77	8.95	-0.37
73	-14.74	8.989	-0.38				
Normal mode Max	Frequency		Intensity		Frequency		Intensity
	1 A		2 A		1 A		27 A
	13398.17		256602636550144		15771.21		57292804325376
ΔE	-2967.73				-2857.42		
Dipole moment	6.7668				8.2113		